Giant ferroelectric modulation of barrier height and width in multiferroic tunnel junctions

L. N. Jiang [1], Yun-Peng Wang [2], W. Z. Chen,[1] and X. F. Han [1,3,4,*]

[1]*Beijing National Laboratory for Condensed Matter Physics, Institute of Physics, Chinese Academy of Sciences, Beijing 100190, China*
[2]*School of Physics and Electronics, Hunan Key Laboratory for Super-Micro Structure and Ultrafast Process, Central South University, Changsha 410083, China*
[3]*Center of Materials Science and Optoelectronics Engineering, University of Chinese Academy of Sciences, Beijing 100049, China*
[4]*Songshan Lake Materials Laboratory, Dongguan, Guangdong 523808, China*

The high tunneling electroresistance (TER) effect, generally caused by ferroelectric (FE)-modulated barrier height or width, is essential for the applications of multiferroic tunnel junctions in data storage. It is traditionally obtained by distinct electrical screening lengths of electrodes. Interface engineering can enhance the TER effect further. In this work, taking Co-$(TiO_2\text{-}BaO)_N$-Co tunnel junctions as examples, we demonstrate a distinct principle than the screening lengths for designing extraordinary TER effect. We reveal that when the interfacial FE displacement is much larger than that of the FE bulk, it will bend the barrier band near the interface violently, and the interfacial polarization direction pointing to or away from the interface determines whether the energy band rises or falls. The large interfacial Ba-O displacement and its corresponding polarization direction in Co-$BaTiO_3$-Co tunnel junctions can be significantly modulated by the direction of FE polarization, resulting in a metallic-insulating transition of the entire thin $BaTiO_3$ barrier. For thick $BaTiO_3$ barrier ($N = 25$, ~ 10 nm), the effective tunnel barrier width shifts between about 2 nm and 6.5 nm as the polarization of $BaTiO_3$ switches direction, which can dramatically modulate the tunneling efficiency. This effect shed light on a novel route for enhancing TER through the interface engineering.

I. INTRODUCTION

The multiferroic tunnel junction (MFTJ), composed of two ferromagnetic (FM) electrodes and a ferroelectric (FE) barrier [1–4], is a promising candidate for the next generation data storage devices [5–7] due to their advantages of ultra-low energy consumption, high density, nonvolatile, fast processing, and multiple resistance states. When the FE polarization switches direction, the variation of electrical resistance is called the tunneling electroresistance (TER) effect. A strong TER effect implies better tolerance of reading errors for memory applications.

The TER effect emerges due to the inversion symmetry breaking of tunnel junctions. One route is to employ two metal electrodes with distinct screening lengths [8–12]. They will produce different screening potentials at two FE barrier-electrode interfaces, and make the barrier height raise or reduce with polarization reversal, thus leading to the TER effect. The other route to break the inversion symmetry is interface engineering. One can insert a thin dielectric layer to one of the interfaces [13–15], such as the $SrRuO_3/SrTiO_3/BaTiO_3/SrRuO_3$ junction [15]. Fundamentally, this method also adopts different screening lengths on both sides of the FE layer [13,15], leading to FE-modulated barrier height and width of dielectric and insulating layers, thus achieving a TER effect. One can also design different

terminations at the two interfaces of the FE barrier [15–17], such as in the $SrRuO_3/(TiO_2\text{-}BaO)_6/SrRuO_3$ tunnel junction [16]. The distinct interface terminations lead to different interface dipoles, which produce an effective field, thus resulting in asymmetric FE displacements and the TER effect [16]. However, due to the common suppression of the film ferroelectricity by the depolarization field, the interface dipoles are usually not very large, so the expected TER effect in the FE termination method appears modest [15,16].

At the interface with simple metals, the AO-terminated perovskite (ABO_3) barrier exhibits an unexpected large relative displacement and thus an enhanced interface ferroelectricity [18]. The large interface displacement distorts the potential profile at the AO-metal interface, and will produce a considerable modulation of the barrier height and width with polarization reversal, thus resulting in a significantly enhanced TER effect. Furthermore, it can be combined with the common screening length method to produce a much higher TER effect.

In this work, using a Co-$(TiO_2\text{-}BaO)_N$-Co junction with BaO-Co interface as an example, we predict via first-principles calculation a giant FE modulation of effective barrier height and width. The large Ba-O displacement at the BaO-Co interface dramatically alter the interfacial potential profile. For junctions with a thin $BaTiO_3$ (BTO) barrier, the whole barrier presents FE controlled metallic-insulating transition. For junctions with a 10-nm-thick BTO barrier, the width of insulating region increases from 2 nm to 6.5 nm as the FE polarization switches, which guarantees an

*Corresponding author: xfhan@iphy.ac.cn

extraordinary TER effect. Moreover, this phenomenon of the metallic barrier is not limited to the junctions with BaO-Co interface, as long as there is much higher interfacial FE displacement than FE bulk and its corresponding polarization direction points away from the interface.

II. COMPUTATIONAL METHOD

The density functional theory (DFT) calculations were performed by the Vienna *ab initio* simulation package (VASP) [19]. We use the projector augmented wave (PAW) pseudopotential [20,21] to describe the interaction between electrons and nuclei, and use PBEsol generalized gradient approximation (GGA) exchange-correlation potential to describe the exchange correlation between electrons [22]. The cutoff energy for the plane wave is 500 eV. The energy convergence criterium is 1×10^{-5} eV. All atomic coordinates are optimized along the z direction, until the forces on all atoms are less than 0.01 eV/Å. The conjugate-gradient algorithm is used for relaxation ions. A $7 \times 7 \times 1$ Γ-centered k-point mesh and a 0.1 eV Gaussian smearing are used in relaxation. For self-consistent and density of states (DOS) calculation, a $16 \times 16 \times 1$ Γ-centered k-point mesh and a 0.05 eV Gaussian smearing are used. For Co-(TiO$_2$-BaO)$_{20}$-Co (Co-(TiO$_2$-BaO)$_{25}$-Co) tunnel junction, the self-consistent calculation uses a $13 \times 13 \times 1$ ($10 \times 10 \times 1$) Γ-centered k-point mesh and the DOS calculation uses a $14 \times 14 \times 1$ ($13 \times 13 \times 1$) Γ-centered k-point mesh.

In HSE06 calculation of Co-(TiO$_2$-BaO)$_3$-Co system, we use $8 \times 8 \times 1$ Γ-centered k-point mesh and 0.15 eV Gaussian smearing in both self-consistent and DOS calculations. The cutoff energy for plane wave is 500 eV. The energy convergence criterium is 1×10^{-5} eV. It should be noted that the 0.15 eV smearing is relatively large. However, it will not lead to the misjudgment of the metallic BTO introduced later in the article. The calculated results of HSE06 show that the bottom of BTO conduction band is about 0.4 eV lower than the Fermi level. Even after deducting the 0.15 eV, BTO is still metallic. Therefore, the large smearing will not affect our calculation results excessively.

III. RESULTS AND DISCUSSIONS

The relaxed structures of Co-(TiO$_2$-BaO)$_5$-Co MFTJ with opposite polarization directions (hereafter denoted as left for pointing from the BaO-Co to TiO$_2$-Co interface and right otherwise) are shown in Figs. 1(a) and 1(b). Supercells are constructed by aligning the [100] axis of BTO with the [110] axis of body centered cubic (bcc) Co. The in-plane (*xy*-plane) lattice constant a is fixed at 3.906 Å, simulating growth on SrTiO$_3$ substrate. The mismatch is about 2% for both bcc Co ($\sqrt{2} \times 2.82$ Å [23,24]) and BTO (3.99 Å). The out-of-plane lattice constant of bulk BTO is 4.192 Å (c/a ratio ~1.073) and the polarization is 44.8 $\mu C/cm^2$.

The asymmetric (TiO$_2$-BaO)$_5$ barrier has two distinct interfaces with Co electrodes. The left interface is Co-TiO$_2$, which is the most stable interface, similar to Fe/BTO multilayers [25]. The right interface is BaO-Co, which is not as stable as the Co-TiO$_2$ interface. Experimental evidences show that BTO films sometimes tend to maintain complete
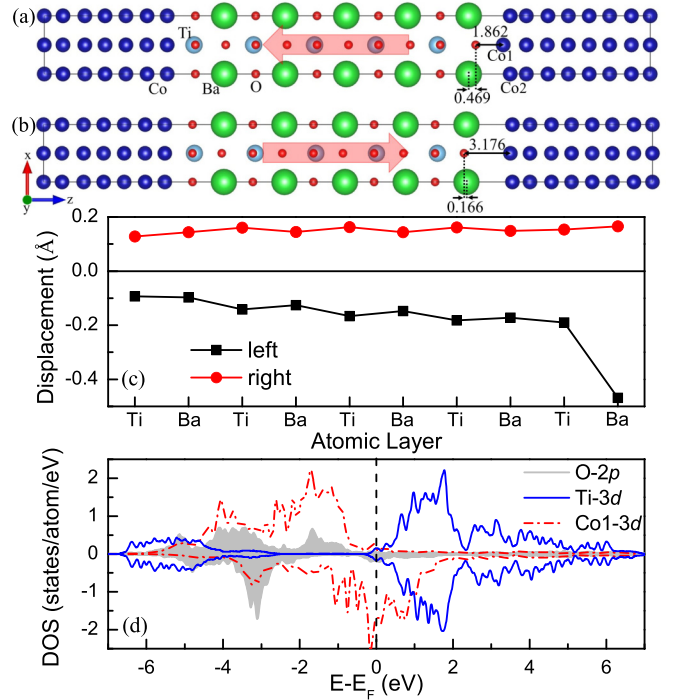

FIG. 1. The structures of Co-(TiO$_2$-BaO)$_5$-Co MFTJ for (a) left polarization and (b) right polarization. Red arrows indicate the polarization direction. The atom distances (unit: Å) at BaO-Co interface are indicated. (c) Ti-O and Ba-O displacements across the left-polarized (black) and right-polarized (red) BTO. (d) Orbital-resolved DOS for O (in BaO layer), Co1, and Ti atoms at the right interface in left-polarized MFTJ.

unit cells, such as (BaO-TiO$_2$)$_N$/Fe [26,27]. Moreover, the calculated separation energy of BaO-Co interface is positive (1.792 J/m^2), similar to SrO-Co and PbO-Co interfaces [28,29]. Therefore, the BaO-Co interface is possible in theory.

The FE displacements across the relaxed BTO barrier are shown in Fig. 1(c). In the right-polarized state, the FE displacements are relatively uniform, about 0.15 Å. In the left-polarized barrier, the amplitude of FE displacements show an increasing trend from the Co-TiO$_2$ to BaO-Co interface, and increases sharply to 0.469 Å at the BaO-Co interface. Our calculation also shows that the distance between adjacent Ba atoms is almost uniform across the left-polarized (TiO$_2$-BaO)$_5$ barrier, while the distance between adjacent O atoms (in BaO layer) has a sudden increase at the right interface. Therefore, the large Ba-O displacement of 0.469 Å mainly comes from the movement of interfacial O atom, which results from O-Co1 hybridization.

The hybridization between Ti-3d and O-2p states is the main source of ferroelectricity of BTO [30]. At the right interface of left-polarized Co-(TiO$_2$-BaO)$_5$-Co MFTJ, as shown in Fig. 1(d), the O-2p (in BaO layer) is slightly hybridized with Ti-3d and strongly hybridized with the Co1-3d state. The hybridization makes the system energy lower when O atom in interfacial BaO layer is close to Ti (right-polarized state) or Co1 (left-polarized state). The Ba atom with the largest ionic radius in the tunnel junction is on hollow of O atom (in the TiO$_2$ layer), but at the bottom of Co2 atom, leading
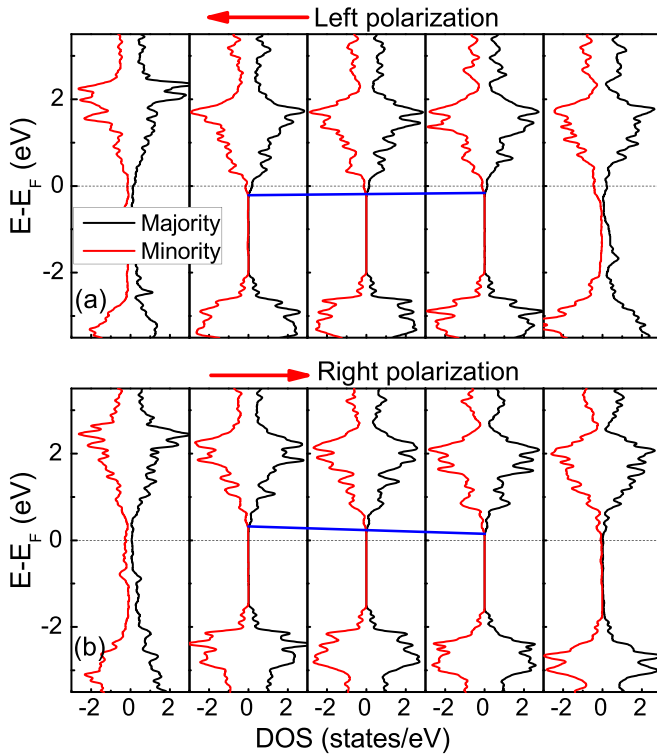
FIG. 2. DOS for each BTO unit cell in Co-$(TiO_2$-$BaO)_5$-Co MFTJ with (a) left-polarized and (b) right-polarized state. Black (red) line is DOS of majority (minority). From left to right, the DOS figures correspond to the BTO unit cell near the Co-TiO_2 interface to near the BaO-Co interface. The dotted line indicates the Fermi level position. The blue solid line connects the CBM of each BTO unit cell.

to a larger layer spacing of BaO-Co than that of TiO_2-BaO. Therefore, the O and Co1 atoms need to move a long distance to approach, accompanied by a considerable interface rumpling and a large Ba-O displacement. The large movement of the interfacial O atom elongates the oxygen octahedron, resulting in an increase in FE polarization. This explains the increasing FE displacements approaching the BaO-Co interface.

The severe (common) distortion of the BaO-Co interface in left (right)-polarized state produces a large (normal) interfacial polarization and hence a large (normal) electrostatic potential change at the right interface, which will greatly modulate the potential profile of BTO by switching the FE polarization. The potential profile is illustrated using the local DOS across the BTO barrier in Fig. 2. For the right-polarized state, the conduction band minimum [CBM, denoted as the blue line in Fig. 2(b)] resides above the Fermi level of the junction, indicating a normal insulating state. As for the left-polarized state, the CBM is lower than the Fermi energy, making the BTO barrier entirely metallic.

The GGA calculation underestimates the band gap of the barrier and thus may mistakenly lead to the special metallic BTO in the left-polarized state. To exclude this factor, we performed GGA $+ U$ and HSE06 hybrid functional calculations. For GGA $+ U$ calculations, the Hubbard parameter is applied on Ti d states. The calculated band gap of BTO

increases from 1.7 eV at $U = 0$ to 2.2 eV at $U = 4$ eV. In the left-polarized Co-$(TiO_2$-$BaO)_N$-Co system ($N = 5$, 10, 15, 20, 25), the enhancement of the band gap from 1.7 eV to 2.2 eV hardly affects the metallicity of BTO. The HSE06 calculations further confirm this point. The HSE06 calculations predict the BTO band gap of 3.0 eV, close to the experimental value of 3.2 eV, and confirm that the BTO barrier is metallic (insulating) in the left (right)-polarized Co-$(TiO_2$-$BaO)_3$-Co system. Increasing the band-gap size close to the experimental value still does not contradict the DFT prediction results.

Generally, based on the electron affinity of BTO ~ 3.9 eV [31] and the work function of Co ~ 5.0 eV, the barrier height between BTO and Co can be estimated to be 1.1 eV, indicating an insulating state. However, there are two factors that produce the band offset of BTO, resulting in the formation of the special metallic BTO. One is the tendency of TiO_2 and BaO terminations to gain and lose electrons, respectively, producing the band offset [32]. Even if the FE displacement of BTO decreases to 0, this effect still works. We test the Co-TiO_2-$(BaO$-$TiO_2)_4$-Co and Co-BaO-$(TiO_2$-$BaO)_4$-Co systems without FE displacement, by performing static calculations. The interface spacing is determined by the total energy minimization. The Bader charge analysis shows that the BTO barrier with two TiO_2 terminations obtains about 0.3799 electrons from electrodes; while the BTO barrier with two BaO terminations loses about 0.0215 electrons to electrodes. As a result, the band of a Co-$(TiO_2$-$BaO)_N$-Co system without FE displacement is tilted. Another factor is the large FE polarization at the interface, which plays a major role in the occurrence of the metallic barrier. Both the magnitude and direction of the interfacial FE polarization should be considered. When its magnitude is much larger than the FE polarization of the bulk, it can greatly change the BTO band. Moreover, its direction determines whether the BTO at the interface gets electrons or loses electrons, pulling down or raising the band near the interface. We do static calculations for the "nonpolar" Co-BaO-$(TiO_2$-$BaO)_4$-Co system, and fix one interfacial BaO displacement to be 0, $+0.1$, $+0.2$, -0.1, and -0.2 Å. Where, the $+ (-)$ represents the interfacial FE polarization pointing away from (to) the interface. The Bader charge analysis shows that BTO loses 0.0215, 0.0358, and 0.0669 electrons for the 0, -0.1, and -0.2 cases, respectively; while BTO obtains 0.019 and 0.057 electrons for the $+0.1$ and $+0.2$ cases, respectively. Therefore, the large interfacial FE polarization pointing away from (to) the interface will bend the band near the corresponding interface to a lower (higher) energy.

To illustrate the specific effect of the two factors on the band offset, we performed three sets of tests. In the first set of tests [Figs. 3(a) to 3(c)], we start from the "nonpolar" Co-$(TiO_2$-$BaO)_{15}$-Co system, and set the interfacial Ba-O displacement to different values. In the second set of tests [Figs. 3(d) to 3(f)], we begin from the polarized Co-$(TiO_2$-$BaO)_{15}$-Co system, and fix the FE displacement of one interface larger than that of the bulk. The relaxation was not performed in the first two groups. In the third test, we carried out the relaxation calculation and verified the conclusions of the first two tests. Please note that the head-to-head and tail-to-tail polarizations are not considered in the tests. We first
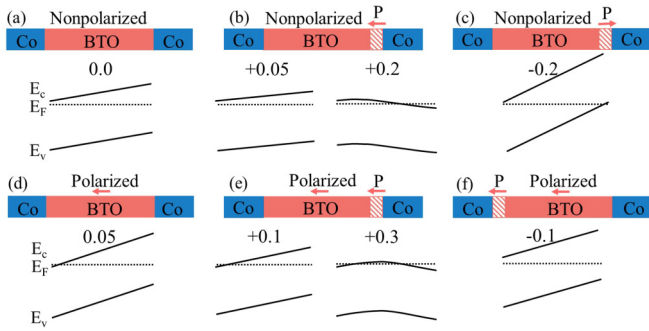
FIG. 3. Schematic diagrams of calculated band structures for Co/(TiO$_2$-BaO)$_{15}$/Co structure with different FE displacement. Interfacial FE displacement is set to (a) 0.0, (b) +0.05, +0.2 Å, and (c) −0.2 Å, while other layers are all 0. The interfacial FE displacement is set to (d) 0.05 Å, (e) +0.1, +0.3 Å, and (f) −0.1 Å, while other layers are all 0.05 Å. The red arrows indicate the polarization direction. + (−) represents the interfacial FE polarization pointing away from (to) the corresponding interface. The interface spacing is determined by the total energy minimization.

analyze the results of the first set of tests. As schematically shown in Fig. 3(a), its band is tilted and decreases by 0.6 eV from BaO to TiO$_2$ interface, even without FE displacement. Comparing the results of +0.2 and −0.2 Å in Figs. 3(b) and 3(c), we can find that when the relatively large FE polarization at the interface points away from (to) the Co electrode, the band near the corresponding interface bends to a lower (higher) energy position. In Fig. 3(b), we compare +0.05 and +0.2 Å results. For the +0.05 Å case, compared with Fig. 3(a), its FE polarization produces about 0.35 eV band offset near the BaO-Co interface, making the CBM of BTO slightly close to the Fermi level. For +0.2 Å case, its large interfacial FE polarization makes the BaO interface obtain more electrons, further bending the energy band of interfacial BTO to a lower energy, which leads to the metallic property of BTO cells near the BaO-Co interface. The thickness of metallic BTO is about 2.4 nm. Based on this, we can draw three conclusions. (1) When the interfacial polarization is much larger than the bulk polarization, it can produce considerable band offset at the interface. The rise and fall of interfacial band depend on the large interfacial FE polarization direction pointing to and away from the interface, respectively. (2) The relatively large FE polarization pointing away from interface can lead to metallic BTO, which can exist in BTO to a depth of several nanometers, and the presence of metallic BTO in turn slows down the increase of band offset. (3) The relatively large interfacial FE polarization has the greatest influence on the band offset of its nearby region, but has little effect on the band offset of the other interface. For the second test, the above three conclusions are still valid. As can be seen from Figs. 3(e) and 3(f), comparing the results of +0.1 and −0.1 Å, the relatively large interfacial FE polarization pointing to (away from) the interface also bends the corresponding interfacial band to a higher (lower) energy position. Similar to Fig. 3(b), with the increase of interfacial FE polarization in Fig. 3(e), the corresponding interfacial BTO band bends to a lower energy, and several nanometers of BTO is metallic in the +0.3 Å case. Therefore, the polarized BTO bulk does not

make a qualitative difference to our three conclusions above, but the FE displacement of BTO bulk results in the need for a larger interfacial FE displacement to produce metallic BTO. In the third test, we artificially fix the interfacial Ti-O displacement at 0.3 Å in right-polarized Co-(TiO$_2$-BaO)$_5$-Co MFTJ, and then relax the MFTJ under this constraint. We fix the interfacial Ti-O displacement at 0.3 Å because it is larger than that of the BTO bulk and its direction of FE polarization points away from the Co-TiO$_2$ interface in the right-polarized state. The results show that the original insulating BTO is transformed into metallic BTO in the entire BTO region. This proves once again that the metallic BTO can be induced by the interfacial FE polarization which is much larger than the bulk polarization and points away from the corresponding interface.

In the left-polarized Co-(TiO$_2$-BaO)$_5$-Co MFTJ [shown in Fig. 1(a)], the interfacial Ba-O displacement is as large as 0.469 Å, which is much larger than the FE displacement in the bulk. Furthermore, its FE polarization direction points away from the BaO-Co interface. It will move the energy band of BTO violently to a lower energy, leading to a metallic BTO. In the right-polarized Co-(TiO$_2$-BaO)$_5$-Co MFTJ [shown in Fig. 1(b)], there is no interface FE displacement much higher than that of the bulk. The influence of interface on the BTO band is very weak. Therefore, the right-polarized BTO presents a normal insulating state.

The polarization-controlled metallic-insulating transition of the BTO barrier can, in principle, be used for controlling the junction resistance using electric fields, thus for designing an electroresistance device. However, the transition from the metallic state to the insulating state remains an issue: free electrons within the metallic BTO barrier region screen the external electric field and forbid the reversal of FE polarization. As will be discussed below, this issue can be resolved by using thicker BTO barrier.

A thick BTO barrier in left-polarized Co-(TiO$_2$-BaO)$_N$-Co junction is not entirely metallic but partial insulating because the metallicity in the left-polarized state is caused by the influence of interface as studied above. For a sufficiently thick BTO barrier, the deeply buried part of the BTO barrier remains insulating, allowing the external electric field to switch the direction of FE polarization. We performed calculations on the left-polarized Co-(TiO$_2$-BaO)$_N$-Co junctions, with the thickness of BTO barrier N increasing from 10 to 25. The calculated electronic structure, namely, the positions of conduction and valence band edges are illustrated in Fig. 4. These data are obtained by sorting out the DOS for each BTO unit cell. Generally, the band of the ferroelectrics should be oblique and decrease in the direction of FE polarization. However, as illustrated in Fig. 4, the interfacial effect produces severe band bending near the right (BaO-Co) interface. Away from the interfaces, the conduction band bends towards the Fermi energy and tends to recover the insulating state of bulk BTO. When the left-polarized barrier is not sufficiently thick ($N < 25$), the BTO barrier remains metallic. For $N = 25$ (about 10 nm), the central part of the BTO barrier becomes insulating with the conduction band edge above the Fermi energy. The insulating region is only about 2-nm thick in the left-polarized state, which allows a high probability of tunneling. This narrow insulating region preserve the tunability
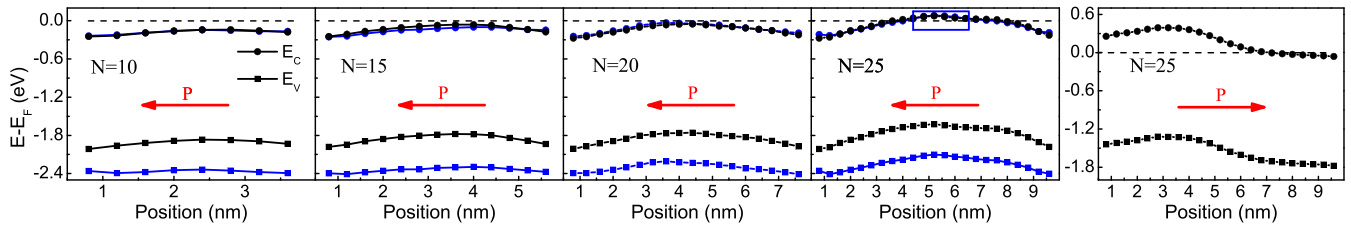
FIG. 4. Fermi level relative to the band edges in the BTO layer in left-polarized Co-(TiO$_2$-BaO)$_N$-Co MFTJs, where $N = 10$, 15, 20, 25, and in right-polarized Co-(TiO$_2$-BaO)$_{25}$-Co MFTJs. Two interfacial BTO cells are not considered here. E_c, E_v and the horizontal dotted line represent the conduction band edge, valence band edge, and the Fermi level, respectively. The black and blue lines represent the data of DFT and DFT $+ U$ ($U = 4$ eV), respectively. Red arrows indicate the FE polarization direction. The insulating region for left-polarized (TiO$_2$-BaO)$_{25}$ is marked by the blue frame.

of polarization direction using electric fields. In the right-polarized state, the effective insulating region is about 6.5 nm, and quantum tunneling will hardly occur with such a thick insulation. Therefore, the metallic-to-insulating transition in thin-barrier junctions turns to a transition between states with distinct widths of insulating regions. By using a thicker FE barrier, we can not only achieve electric-field modulations, but also dramatically regulate the tunneling efficiency to obtain a significant TER effect.

The predicted principle of interface enhanced TER can be reproduced in many structures with a larger FE displacement than the bulk at the interface. When we replace the bcc Co electrode with bcc Fe or bcc Ni, there is also a large interfacial Ba-O displacement and FE controlled metallic-insulating transition in tunnel junctions with thin BTO barrier. (Some representative data of Co/BTO/Co and Fe/BTO/Fe systems are included in the Supplemental Materials [33]). Furthermore, the predicted principle can also be combined with the common screening length method. We tried to use SrRuO$_3$ as the left electrode, but keep the right BaO-Co interface unchanged. Calculations confirm that the entire BTO barriers inside both SrRuO$_3$/(TiO$_2$-BaO)$_5$/Co and SrRuO$_3$/BaO-(TiO$_2$-BaO)$_5$/Co junctions are metallic when the FE polarization points from Co to SrRuO$_3$ electrode. With FE polarization reversal, the insulation of BTO in the two junctions recovers. Moreover, the metallic barrier can also be induced by the TiO$_2$-metal interface. For example, a relatively large interfacial TiO$_2$ displacement with corresponding polarization pointing away from the FeSi-TiO$_2$ interface in Co$_2$FeSi/(TiO$_2$-BaO)$_5$/SrRuO$_3$ tunnel junction leads to a metallic barrier. Therefore, the results for the Co/BTO/Co junctions can be extended to many junctions. This principle paves the way for designing efficient ferroelectric or multiferroic tunnel junctions.

[1] V. Garcia, M. Bibes, L. Bocher, S. Valencia, F. Kronast, A. Crassous, X. Moya, S. Enouz-Vedrenne, A. Gloter, D. Imhoff, C. Deranlot, N. D. Mathur, S. Fusil, K. Bouzehouane, and A. Barthélémy, Science **327**, 1106 (2010).

[2] D. Pantel, S. Goetze, D. Hesse, and M. Alexe, Nat. Mater. **11**, 289 (2012).

[3] G. Sanchez-Santolino, J. Tornos, D. Hernandez-Martin, J. I. Beltran, C. Munuera, M. Cabero, A. Perez-Muñoz, J. Ricote, F. Mompean, M. Garcia-Hernandez, Z. Sefrioui, C. Leon, S. J. Pennycook, M. C. Muñoz, M. Varela, and J. Santamaria, Nat. Nanotech. **12**, 655 (2017).

[4] J. Tornos, F. Gallego, S. Valencia, Y. H. Liu, V. Rouco, V. Lauter, R. Abrudan, C. Luo, H. Ryll, Q. Wang, D. Hernandez-Martin, G. Orfila, M. Cabero, F. Cuellar, D. Arias, F. J. Mompean, M. Garcia-Hernandez, F. Radu, T. R. Charlton, A. Rivera-Calzada, Z. Sefrioui, S. G. E. te Velthuis, C. Leon, and J. Santamaria, Phys. Rev. Lett. **122**, 037601 (2019).

[5] J. F. Scott, Nat. Mater. **6**, 256 (2007).

[6] F. Yang, M. H. Tang, Z. Ye, Y. C. Zhou, X. J. Zheng, J. X. Tang, and J. J. Zhang, J. Appl. Phys. **102**, 044504 (2007).

[7] J. J. Ruan, C. Li, Z. S. Yuan, P. Wang, A. D. Li, and D. Wu, Appl. Phys. Lett. **109**, 252903 (2016).

[8] M. Ye. Zhuravlev, R. F. Sabirianov, S. S. Jaswal, and E. Y. Tsymbal, Phys. Rev. Lett. **94**, 246802 (2005).

[9] Z. Wen, C. Li, D. Wu, A. D. Li, and N. B. Ming, Nat. Mater. **12**, 617 (2013).

[10] A. Quindeau, V. Borisov, I. Fina, S. Ostanin, E. Pippel, I. Mertig, D. Hesse, and M. Alexe, Phys. Rev. B **92**, 035130 (2015).

[11] X. Liu, J. D. Burton, and E. Y. Tsymbal, Phys. Rev. Lett. **116**, 197602 (2016).

[12] C. Ma, Z. Luo, W. C. Huang, L. T. Zhao, Q. L. Chen, Y. Lin, X. Liu, Z. W. Chen, C. C. Liu, H. Y. Sun, X. Jin, Y. W. Yin, and X. G. Li, Nat. Commun. **11**, 1439 (2020).

[13] M. Ye. Zhuravlev, Y. Wang, S. Maekawa, and E. Y. Tsymbal, Appl. Phys. Lett. **95**, 052902 (2009).

[14] A. Tsurumaki-Fukuchi, H. Yamada, and A. Sawa, Appl. Phys. Lett. **103**, 152903 (2013).

[15] N. M. Caffrey, T. Archer, I. Rungger, and S. Sanvito, Phys. Rev. Lett. **109**, 226803 (2012).

[16] J. P. Velev, C. G. Duan, J. D. Burton, A. Smogunov, M. K. Niranjan, E. Tosatti, S. S. Jaswal, and E. Y. Tsymbal, Nano Lett. **9**, 427 (2009).

[17] L. L. Tao and J. Wang, Appl. Phys. Lett. **108**, 062903 (2016).

[18] M. Stengel, D. Vanderbilt, and N. A. Spaldin, Nat. Mater. **8**, 392 (2009).

[19] G. Kresse and J. Furthmüller, Phys. Rev. B **54**, 11169 (1996).

[20] P. E. Blöchl, Phys. Rev. B **50**, 17953 (1994).

[21] G. Kresse and D. Joubert, Phys. Rev. B **59**, 1758 (1999).

[22] J. P. Perdew, A. Ruzsinszky, G. I. Csonka, O. A. Vydrov, G. E. Scuseria, L. A. Constantin, X. Zhou, and K. Burke, Phys. Rev. Lett. **100**, 136406 (2008).

[23] G. A. Prinz, Phys. Rev. Lett. **54**, 1051 (1985).

[24] R. Walmsley, J. Thompson, D. Friedman, R. M. White, and T. H. Geballe, IEEE Trans. Magn. **19**, 1992 (1983).

[25] C.-G. Duan, S. S. Jaswal, and E. Y. Tsymbal, Phys. Rev. Lett. **97**, 047201 (2006).

[26] H. L. Meyerheim, F. Klimenta, A. Ernst, K. Mohseni, S. Ostanin, M. Fechner, S. Parihar, I. V. Maznichenko, I. Mertig, and J. Kirschner, Phys. Rev. Lett. **106**, 087203 (2011).

[27] H. L. Meyerheim, A. Ernst, K. Mohseni, I. V. Maznichenko, J. Henk, S. Ostanin, N. Jedrecy, F. Klimenta, J. Zegenhagen, C. Schlueter, I. Mertig, and J. Kirschner, Phys. Rev. Lett. **111**, 105501 (2013).

[28] I. I. Oleinik, E. Y. Tsymbal, and D. G. Pettifor, Phys. Rev. B **65**, 020401(R) (2001).

[29] V. S. Borisov, S. Ostanin, S. Achilles, J. Henk, and I. Mertig, Phys. Rev. B **92**, 075137 (2015).

[30] R. E. Cohen, Nature (London) **358**, 136 (1992).

[31] T. J. Zhang, R. K. Pan, Z. J. Ma, M. G. Duan, D. F. Wang, and M. He, Appl. Phys. Lett. **99**, 182106 (2011).

[32] L. N. Jiang, W. Z. Chen, B. S. Yang, X.-G. Zhang, Y.-P. Wang, and X. F. Han, Phys. Rev. B **99**, 224103 (2019).

[33] See Supplemental Material at http://link.aps.org/supplemental/10.1103/PhysRevB.103.214441 for more information on these materials.

[34] K. Momma and F. Izumi, J. Appl. Crystallogr. **44**, 1272 (2011).